ASME 2012 5th Annual Dynamic Systems and Control Conference joint with the JSME 2012 11th Motion and Vibration Conference
DSCC2012-MOVIC2012
October 17-19, 2012, Fort Lauderdale, Florida, USA

DSCC2012-MOVIC2012-8573

ADAPTIVE CONTROL OF UNCERTAIN LINEAR SYSTEMS WITH UNCERTAIN HYSTERETIC INPUT NONLINEARITIES

M. Al Janaideh, D. Sumer, J. Yan, A. M. D'Amato, B. Drincic, K. Aljanaideh, and D. S. Bernstein

Department of Aerospace Engineering
The University of Michigan
Ann Arbor MI 48109 *

ABSTRACT

We apply retrospective cost adaptive control (RCAC) with auxiliary nonlinearities to a command-following problem for uncertain Hammerstein systems with rate-dependent hysteretic input nonlinearities. The only required modeling information of the linear plant is a single Markov parameter. To account for the hysteretic input nonlinearity, RCAC uses auxiliary nonlinearities that reflect the monotonicity properties of the input nonlinearity. The hysteresis nonlinearity is modeled using the rate-dependent Prandtl-Ishlinskii model.

1 INTRODUCTION

Smart actuators, such as devices based on piezoelectric and magnetostrictive materials, use electrical energy to realize large strains and forces [1]. These devices enable control for a wide range of new applications [2, 3]. Using these actuators for control applications is challenging, however, due to the fact that these materials are hysteretic [4]. Consequently, the closed-loop system may exhibit oscillatory closed-loop behavior, as well as poor tracking and potential instability. The effect of hysteresis nonlinearities tends to become more pronounced under high input rates [5].

The most direct approach to dealing with hysteresis is to invert the nonlinearity [6, 7]. When the hysteresis map is uncertain, the hysteresis can be inverted robustly or adaptively [8]. For simplicity, a rate-independent inverse hysteresis can be used. However, rate-independent inverse hysteresis neglects the effect of the input rate and may cause compensation errors [9]. Adaptive control can also be used without hysteresis inversion [10].

Systems with hysteretic actuators can be viewed as a special class of Hammerstein systems, in which an input nonlinearity precedes the linear dynamics of the plant. The nonlinearity in a Hammerstein system may be a saturation function to reflect magnitude restrictions on the control input, as well as a deadzone or relay nonlinearity.

In applications such as closed-loop micro-positioning systems it is necessary to compensate for hysteresis effects to enhance the tracking performance of smart actuators. The hysteresis properties of such actuators may be highly nonlinear functions of the magnitude and rate of change of the input. Consequently, modeling and controlling these devices presents considerable challenges. In the present paper we consider the problem of controlling a Hammerstein plant with a hysteretic input nonlinearity. We assume that the hysteretic input nonlinearity is uncertain, and thus we do not attempt to compensate for it by using inversion. Instead, we apply retrospective-cost adaptive control (RCAC), which can be used for plants that are possibly MIMO, nonminimum-phase (NMP), and unstable [11–15]. For SISO plants, this approach requires knowledge of a single nonzero Markov parameter and can compensate for the presence of nonminimum-phase zeros, as shown in [16, 17]. In [18], RCAC is applied to Hammerstein systems with memoryless nonlinearities.

In the present paper we focus on hysteretic nonlinearities modeled by the Prandtl-Ishlinskii model, which is a phenomenological operator-based hysteresis model. This model has been used to characterize rate-independent and rate-dependent hysteresis nonlinearities in smart actuators [5, 19].

*M. Al Janaideh is with the Department of Mechatronics Engineering, The University of Jordan, Amman 11942, Jordan. The remaining authors are with the Department of Aerospace Engineering, The University of Michigan, Ann Arbor, MI 48109.

2 HAMMERSTEIN COMMAND-FOLLOWING PROBLEM

Consider the SISO discrete-time Hammerstein system

$$x(k+1) = Ax(k) + B\mathcal{N}(u(k)) + D_1 w(k), \tag{1}$$
$$y(k) = Cx(k), \tag{2}$$

where $x(k) \in \mathbb{R}^n$, $u(k) \in \mathbb{R}$, $w(k) \in \mathbb{R}$, $\mathcal{N} : \mathbb{R} \to \mathbb{R}$, and $k \geq 0$. We consider the Hammerstein command-following problem with

$$z(k) = y(k) - r(k), \tag{3}$$

where $y(k)$, $z(k)$, $r(k) \in \mathbb{R}$. The goal is to develop an adaptive output feedback controller that minimizes the command-following error z with minimal modeling information about the dynamics, disturbance w, and the input nonlinearity $\mathcal{N}$. We assume that measurements of $z(k)$ are available for feedback; however, measurements of $v = \mathcal{N}(u)$ are not available. The block diagram for (1)-(3) is shown in Figure 1.

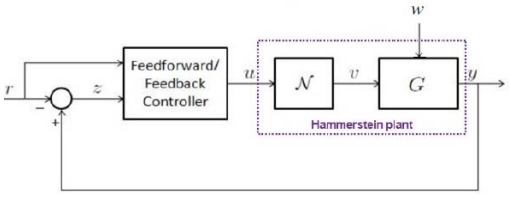

Figure 1. Adaptive command-following problem for a Hammerstein plant. We assume that measurements of $z(k)$ are available for feedback; however, measurements of $v = \mathcal{N}(u)$ and $w(k)$ are not available. The feedforward path is optional.

3 ADAPTIVE CONTROL FOR THE HAMMERSTEIN COMMAND-FOLLOWING PROBLEM

For the Hammerstein command-following problem, we assume that G is uncertain except for an estimate of a single nonzero Markov parameter. The input nonlinearity $\mathcal{N}$ is also uncertain; the required modeling information for $\mathcal{N}$ is specified below. To account for the presence of the input nonlinearity $\mathcal{N}$, the RCAC controller in Figure 2 uses two auxiliary nonlinearities. The auxiliary nonlinearity $\mathcal{N}_1$ modifies u_c to obtain the regressor input u_r, while the auxiliary nonlinearity $\mathcal{N}_2$ modifies the RCAC controller output u_r to produce the Hammerstein plant input u. The auxiliary nonlinearities $\mathcal{N}_1$ and $\mathcal{N}_2$ are chosen based on limited knowledge of the input nonlinearity $\mathcal{N}$, as described below.

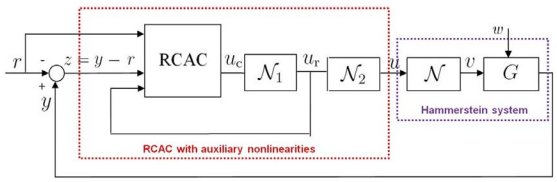

Figure 2. Hammerstein command-following problem with the RCAC adaptive controller and auxiliary nonlinearities $\mathcal{N}_1$ and $\mathcal{N}_2$. The auxiliary nonlinearities are constructed based on limited knowledge of $\mathcal{N}$.

3.1 Auxiliary Nonlinearity $\mathcal{N}_1$

Define the saturation function sat_a by

$$\mathcal{N}_1(u_c) = \mathrm{sat}_a(u_c) = \begin{cases} -a, & \text{if} \quad u_c < -a, \\ u_c, & \text{if} \quad -a \leq u_c \leq a, \\ a, & \text{if} \quad u_c > a, \end{cases} \tag{4}$$

where $a > 0$ is the saturation level. For minimum-phase plants, the auxiliary nonlinearity $\mathcal{N}_1$ is not needed, and thus the saturation level a is chosen to be a large number. For NMP plants, the saturation level a is chosen to tune the transient behavior. In addition to the transient behavior, the saturation level is chosen based on the magnitude of the control input needed to follow the command r. This level depends on the range of the input nonlinearity $\mathcal{N}$ as well as the gain of the linear system G at frequencies in the spectrum of r.

3.2 Auxiliary Nonlinearity $\mathcal{N}_2$

To construct $\mathcal{N}_2$, we assume that the intervals of monotonicity of the input nonlinearity $\mathcal{N}$ are known; no further modeling information about $\mathcal{N}$ is needed. Let $I_1, I_2, \ldots$ be intervals that partition the real numbers. If $\mathcal{N}$ is nondecreasing on I_i, then $\mathcal{N}_2(u_r) = u_r$ for all $u_r \in I_i$. Alternatively, if $\mathcal{N}$ is nonincreasing on $I_i = (p_i, q_i)$, then $\mathcal{N}_2(u_r) = p_i + q_i - u_r \in I_i$ for all $u_r \in I_i$. Finally, if $\mathcal{N}$ is constant on I_i, then either choice can be used. Let $\mathcal{R}_a(f)$ denote the range of the function f with arguments in [-a,a].

Proposition 3.1. Assume that $\mathcal{N}_2$ is constructed by the above rule. Then the following statements hold:

i) $\mathcal{N} \circ \mathcal{N}_2$ is piecewise nondecreasing.
ii) $\mathcal{R}_a(\mathcal{N} \circ \mathcal{N}_2) = \mathcal{R}_a(\mathcal{N})$.

Proof. Let $I_i = (p_i, q_i)$. We first assume that $\mathcal{N}$ is nondecreasing on I_i. Since $\mathcal{N}_2(u_r) = u_r$ for all $u_r \in I_i$, it follows that $\mathcal{N} \circ \mathcal{N}_2(u_r) = \mathcal{N}(u_r)$ for all $u_r \in I_i$. Hence $\mathcal{N} \circ \mathcal{N}_2$ is nondecreasing on I_i. Next, assume that $\mathcal{N}$ is nonincreasing on I_i. Let $u_{r,1}, u_{r,2} \in I_i$, where $u_{r,1} \leq u_{r,2}$. Since $\mathcal{N}_2(u_r) = p_i + q_i - u_r$ for all $u_r \in I_i$, it follows that

$$u_2 \stackrel{\triangle}{=} p_i + q_i - u_{r,2} \leq u_1 \stackrel{\triangle}{=} p_i + q_i - u_{r,1}.$$

Therefore, since $\mathcal{N}$ is nonincreasing on I_i, it follows that $\mathcal{N}(\mathcal{N}_2(u_{\mathrm{r},1})) = \mathcal{N}(u_1) \leq \mathcal{N}(u_2) = \mathcal{N}(\mathcal{N}_2(u_{\mathrm{r},2}))$. Thus, $\mathcal{N} \circ \mathcal{N}_2$ is nondecreasing on I_i.

Finally, to prove *ii*), assume that $\mathcal{N}$ is nondecreasing on I_i. Since $\mathcal{N}_2(u_{\mathrm{r}}) = u_{\mathrm{r}}$ for all $u_{\mathrm{r}} \in I_i$, it follows that $\mathcal{N}_2(I_i) = I_i$, that is, $\mathcal{N}_2 : I_i \to I_i$ is onto. Alternatively, assume that $\mathcal{N}$ is nonincreasing on I_i. Then $\mathcal{N}_2(u_{\mathrm{r}}) = p_i + q_i - u_{\mathrm{r}} \in I_i$. Let $y = \mathcal{N}_2(u_{\mathrm{r}})$ be an element of the codomain, consider $y = p_i + q_i - u_{\mathrm{r}}$, and solve for u_{r} yields $u_{\mathrm{r}} = p_i + q_i - y$. Thus, for all $y \in I_i$, there exists $p_i + q_i - y \in I_i$ such that $\mathcal{N}_2(p_i + q_i - y) = y$. Therefore, $\mathcal{N}_2 : I_i \to I_i$ is onto. Hence, $\mathcal{R}_a(\mathcal{N} \circ \mathcal{N}_2) = \mathcal{R}_a(\mathcal{N})$. □

Example 3.1. Consider the input nonlinearity $\mathcal{N}(u) = -\mathrm{sat}(\Psi[u])$ with $u(t) = 2\sin(2\pi t)$. For each interval of a partition $0 = t_0 < t_1 < \cdots < t_l = 10$, the output of the play operator for $t \in [t_{j-1}, t_j]$ expressed as

$$\Psi[u](t) = \max\{u(t) - 0.5, \min\{u(t) + 0.5, \Psi[u](t_{j-1})\}\}.$$

The input nonlinearity $\mathcal{N}(u) = -\mathrm{sat}(\Psi[u])$ is nonincreasing for all $u \in \mathcal{R}_a$ as shown in Figure 3(a). Let $\mathcal{N}_2(u_{\mathrm{r}}) = -u_{\mathrm{r}}$ according to Proposition 3.1. Figure 3(c) shows that the composite nonlinearity $\mathcal{N} \circ \mathcal{N}_2$ is nondecreasing. Note that $\mathcal{R}_2(\mathcal{N} \circ \mathcal{N}_2) = \mathcal{R}_2(\mathcal{N})$.

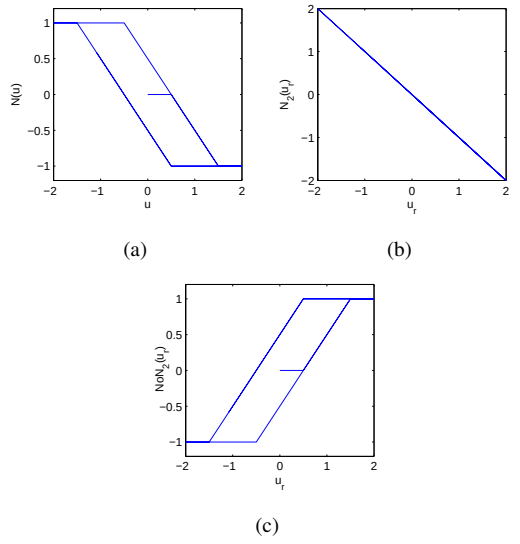

(a) (b) (c)

Figure 3. Example 3.1 (a) Input nonlinearity $\mathcal{N}(u) = -\mathrm{sat}(\Psi[u])$, (b) Auxiliary nonlinearity $\mathcal{N}_2(u_{\mathrm{r}})$ given by (6), and (c) The composite nonlinearity $\mathcal{N} \circ \mathcal{N}_2$. Note that $\mathcal{N} \circ \mathcal{N}_2$ is piecewise nondecreasing and $\mathcal{R}_2(\mathcal{N} \circ \mathcal{N}_2) = \mathcal{R}_2(\mathcal{N})$.

Example 3.2. Consider $u(t) = 2\sin(2\pi t)$ and input nonlinearity shown in Figure 4(a), which is given by

$$\mathcal{N}(u) = \begin{cases} -\mathrm{sat}_{0.5}(\Psi[u]), & \text{if } -2 \leq u \leq 1, \\ \frac{u^2}{5} - 0.7, & \text{if } 1 < u \leq 2. \end{cases} \tag{5}$$

We use $\Psi[u]$ considered in Example (3.1). Let

$$\mathcal{N}_2(u_{\mathrm{r}}) = \begin{cases} -u_{\mathrm{r}}, & \text{if } -2 \leq u \leq 1, \\ u_{\mathrm{r}}, & \text{if } 1 < u \leq 2, \end{cases} \tag{6}$$

according to Proposition 3.1. Figure 4(c) shows that the composite nonlinearity $\mathcal{N} \circ \mathcal{N}_2$ is piecewise nondecreasing. Note that $\mathcal{R}_2(\mathcal{N} \circ \mathcal{N}_2) = \mathcal{R}_2(\mathcal{N})$.

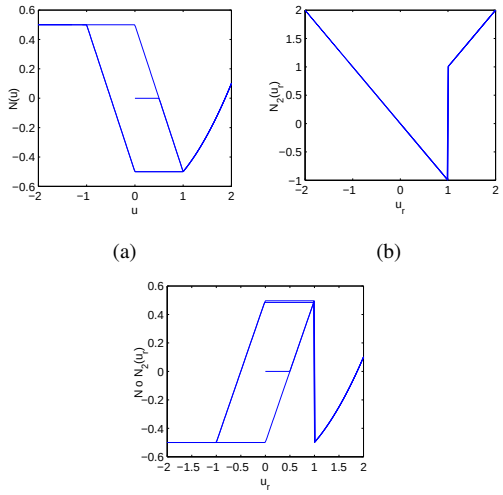

(a) (b) (c)

Figure 4. Example 3.2 (a) Input nonlinearity $\mathcal{N}(u)$ (5), (b) Auxiliary nonlinearity $\mathcal{N}_2(u_{\mathrm{r}})$ given by (6), and, (c) The composite nonlinearity $\mathcal{N} \circ \mathcal{N}_2$. Note that $\mathcal{N} \circ \mathcal{N}_2$ is piecewise nondecreasing and $\mathcal{R}_2(\mathcal{N} \circ \mathcal{N}_2) = \mathcal{R}_2(\mathcal{N})$.

Knowledge of only the intervals of monotonicity of $\mathcal{N}$ is needed to modify the controller output u_{r} such that the composite nonlinearity $\mathcal{N} \circ \mathcal{N}_2$ is piecewise nondecreasing. It thus follows that the known Markov parameters $\tilde{H}$ of G capture correct sign information of the linearized Markov parameters for the Hammerstein system since $\mathcal{N} \circ \mathcal{N}_2$ is piecewise nondecreasing. For details, see [17].

4 Retrospective-Cost Adaptive Control

For $i \geq 1$, define the Markov parameter

$$H_i \triangleq E_1 A^{i-1} B.$$

For example, $H_1 = E_1 B$ and $H_2 = E_1 AB$. Let ℓ be a positive integer. Then, for all $k \geq \ell$,

$$x(k) = A^{\ell} x(k-\ell) + \sum_{i=1}^{\ell} A^{i-1} B \mathcal{N}(\mathcal{N}_2(\mathcal{N}_1(u_{\mathrm{c}}(k-i)))), \tag{7}$$

and thus

$$z(k) = E_1 A^{\ell} x(k-\ell) - E_0 r(k) + \bar{H}\bar{U}(k-1), \tag{8}$$

where

$$\bar{H} \triangleq \begin{bmatrix} H_1 & \cdots & H_\ell \end{bmatrix} \in \mathbb{R}^{l_z \times \ell l_u}$$

and

$$\bar{U}(k-1) \triangleq \begin{bmatrix} \mathcal{N}(\mathcal{N}_2(\mathcal{N}_1(u_c(k-1)))) \\ \vdots \\ \mathcal{N}(\mathcal{N}_2(\mathcal{N}_1(u_c(k-\ell)))) \end{bmatrix}.$$

Next, we rearrange the columns of $\bar{H}$ and the components of $\bar{U}(k-1)$ and partition the resulting matrix and vector so that

$$\bar{H}\bar{U}(k-1) = \mathcal{H}'U'(k-1) + \mathcal{H}U(k-1), \tag{9}$$

where $\mathcal{H}' \in \mathbb{R}^{l_z \times (\ell l_u - l_U)}$, $\mathcal{H} \in \mathbb{R}^{l_z \times l_U}$, $U'(k-1) \in \mathbb{R}^{\ell l_u - l_U}$, and $U(k-1) \in \mathbb{R}^{l_U}$. Then, we can rewrite (8) as

$$z(k) = \mathcal{S}(k) + \mathcal{H}U(k-1), \tag{10}$$

where

$$\mathcal{S}(k) \triangleq E_1 A^{\ell} x(k-\ell) - E_0 r(k) + \mathcal{H}'U'(k-1). \tag{11}$$

Next, for $j = 1, \ldots, s$, we rewrite (10) with a delay of k_j time steps, where $0 \le k_1 \le k_2 \le \cdots \le k_s$, in the form

$$z(k-k_j) = \mathcal{S}_j(k-k_j) + \mathcal{H}_j U_j(k-k_j-1), \tag{12}$$

where (11) becomes

$$\mathcal{S}_j(k-k_j) \triangleq E_1 A^{\ell} x(k-k_j-\ell) + \mathcal{H}_j'U_j'(k-k_j-1)$$

and (9) becomes

$$\bar{H}\bar{U}(k-k_j-1) = \mathcal{H}_j'U_j'(k-k_j-1) + \mathcal{H}_j U_j(k-k_j-1),$$

where $\mathcal{H}_j' \in \mathbb{R}^{l_z \times (\ell l_u - l_{U_j})}$, $\mathcal{H}_j \in \mathbb{R}^{l_z \times l_{U_j}}$, $U_j'(k-k_j-1) \in \mathbb{R}^{\ell l_u - l_{U_j}}$, and $U_j(k-k_j-1) \in \mathbb{R}^{l_{U_j}}$. Now, by stacking $z(k-k_1), \ldots, z(k-k_s)$, we define the *extended performance*

$$Z(k) \triangleq \begin{bmatrix} z(k-k_1) \\ \vdots \\ z(k-k_s) \end{bmatrix} \in \mathbb{R}^{sl_z}. \tag{13}$$

Therefore,

$$Z(k) \triangleq \tilde{\mathcal{S}}(k) + \tilde{\mathcal{H}}\tilde{U}(k-1), \tag{14}$$

where

$$\tilde{\mathcal{S}}(k) \triangleq \begin{bmatrix} \mathcal{S}_1(k-k_1) \\ \vdots \\ \mathcal{S}_s(k-k_s) \end{bmatrix} \in \mathbb{R}^{sl_z},$$

$\tilde{U}(k-1)$ has the form

$$\tilde{U}(k-1) \triangleq \begin{bmatrix} \mathcal{N}(\mathcal{N}_2(\mathcal{N}_1(u_c(k-q_1)))) \\ \vdots \\ \mathcal{N}(\mathcal{N}_2(\mathcal{N}_1(u_c(k-q_{l_{\tilde{U}}})))) \end{bmatrix} \in \mathbb{R}^{l_{\tilde{U}}},$$

where, for $i = 1, \ldots, l_{\tilde{U}}$, $k_1 \le q_i \le k_s + \ell$, and $\tilde{\mathcal{H}} \in \mathbb{R}^{sl_z \times l_{\tilde{U}}}$ is constructed according to the structure of $\tilde{U}(k-1)$. The vector $\tilde{U}(k-1)$ is formed by stacking $U_1(k-k_1-1), \ldots, U_s(k-k_s-1)$ and removing copies of repeated components. Next, we define the *retrospective performance*

$$\hat{z}(k-k_j) \triangleq \mathcal{S}_j(k-k_j) + \mathcal{H}_j\hat{U}_j(k-k_j-1), \tag{15}$$

where the past controls $U_j(k-k_j-1)$ in (12) are replaced by the surrogate controls $\hat{U}_j(k-k_j-1)$.

In analogy with (13), the *extended retrospective performance* for (15) is defined as

$$\hat{Z}(k) \triangleq \begin{bmatrix} \hat{z}(k-k_1) \\ \vdots \\ \hat{z}(k-k_s) \end{bmatrix} \in \mathbb{R}^{sl_z}$$

and thus is given by

$$\hat{Z}(k) = \tilde{\mathcal{S}}(k) + \tilde{\mathcal{H}}\hat{\tilde{U}}(k-1), \tag{16}$$

where the components of $\hat{\tilde{U}}(k-1) \in \mathbb{R}^{l_{\tilde{U}}}$ are the components of

$\hat{U}_1(k-k_1-1),\ldots,\hat{U}_s(k-k_s-1)$ ordered in the same way as the components of $\tilde{U}(k-1)$. Subtracting (14) from (16) yields

$$\hat{Z}(k) = Z(k) - \tilde{\mathcal{H}}\tilde{U}(k-1) + \tilde{\mathcal{H}}\hat{\tilde{U}}(k-1). \tag{17}$$

Finally, we define the *retrospective cost function*

$$J(\hat{\tilde{U}}(k-1),k) \triangleq \hat{Z}^{\mathrm{T}}(k)R(k)\hat{Z}(k), \tag{18}$$

where $R(k) \in \mathbb{R}^{l_z s \times l_z s}$ is a positive-definite performance weighting. The goal is to determine refined controls $\hat{\tilde{U}}(k-1)$ that would have provided better performance than the controls $U(k)$ that were applied to the system. The refined control values $\hat{\tilde{U}}(k-1)$ are subsequently used to update the controller. Next, to ensure that (18) has a global minimizer, we consider the regularized cost

$$\bar{J}(\hat{\tilde{U}}(k-1),k) \triangleq \hat{Z}^{\mathrm{T}}(k)R(k)\hat{Z}(k) + \eta(k)\hat{\tilde{U}}^{\mathrm{T}}(k-1)\hat{\tilde{U}}(k-1), \tag{19}$$

where $\eta(k) \geq 0$. Substituting (17) into (19) yields

$$\bar{J}(\hat{\tilde{U}}(k-1),k) = \hat{\tilde{U}}(k-1)^{\mathrm{T}}\mathcal{A}(k)\hat{\tilde{U}}(k-1) + \mathcal{B}(k)\hat{\tilde{U}}(k-1) + \mathcal{C}(k),$$

where

$$\begin{aligned}
\mathcal{A}(k) &\triangleq \tilde{\mathcal{H}}^{\mathrm{T}}R(k)\tilde{\mathcal{H}} + \eta(k)I_{l_{\tilde{U}}},\\
\mathcal{B}(k) &\triangleq 2\tilde{\mathcal{H}}^{\mathrm{T}}R(k)[Z(k) - \tilde{\mathcal{H}}\tilde{U}(k-1)],\\
\mathcal{C}(k) &\triangleq Z^{\mathrm{T}}(k)R(k)Z(k) - 2Z^{\mathrm{T}}(k)R(k)\tilde{\mathcal{H}}\tilde{U}(k-1)\\
&\quad + \tilde{U}^{\mathrm{T}}(k-1)\tilde{\mathcal{H}}^{\mathrm{T}}R(k)\tilde{\mathcal{H}}\tilde{U}(k-1).
\end{aligned}$$

If either $\tilde{\mathcal{H}}$ has full column rank or $\eta(k) > 0$, then $\mathcal{A}(k)$ is positive definite. In this case, $\bar{J}(\hat{\tilde{U}}(k-1),k)$ has the unique global minimizer

$$\hat{\tilde{U}}(k-1) = -\frac{1}{2}\mathcal{A}^{-1}(k)\mathcal{B}(k). \tag{20}$$

The control $u(k)$ is given by the strictly proper time-series controller of order n_{c} given by

$$u(k) = \sum_{i=1}^{n_{\mathrm{c}}} M_i(k)u(k-i) + \sum_{i=1}^{n_{\mathrm{c}}} N_i(k)z(k-i) + \sum_{i=1}^{n_{\mathrm{c}}} Q_i(k)w(k-i), \tag{21}$$

where, for all $i = 1,\ldots,n_{\mathrm{c}}$, $M_i(k) \in \mathbb{R}^{l_u \times l_u}$, $N_i(k) \in \mathbb{R}^{l_u \times l_z}$, and $Q_i(k) \in \mathbb{R}^{l_u \times l_w}$. The control (21) can be expressed as

$$u(k) = \theta(k)\phi(k-1),$$

where

$$\theta(k) \triangleq \begin{bmatrix} M_1(k) & \cdots & M_{n_{\mathrm{c}}}(k) & N_1(k) & \cdots & N_{n_{\mathrm{c}}}(k) & Q_1(k) & \cdots & Q_{n_{\mathrm{c}}}(k) \end{bmatrix} \in \mathbb{R}^{l_u \times n_{\mathrm{c}}(l_u+l_z+l_w)}$$

and

$$\phi(k-1) \triangleq [u(k-1) \cdots u(k-n_{\mathrm{c}})\ z(k-1) \cdots z(k-n_{\mathrm{c}})\ w(k-1) \cdots w(k-n_{\mathrm{c}})]^{\mathrm{T}} \in \mathbb{R}^{n_{\mathrm{c}}(l_u+l_y+l_w)}.$$

Next, let d be a positive integer such that $\tilde{U}(k-1)$ contains $u(k-d)$ and define the cumulative cost function

$$\begin{aligned}
J_{\mathrm{R}}(\theta,k) \triangleq \sum_{i=d+1}^{k} \lambda^{k-i}\|\phi^{\mathrm{T}}(i-d-1)\theta^{\mathrm{T}}(k) - \hat{u}^{\mathrm{T}}(i-d)\|^2\\
+ (\theta(k)-\theta_0)P_0^{-1}(\theta(k)-\theta_0)^{\mathrm{T}},
\end{aligned} \tag{22}$$

where $\|\cdot\|$ is the Euclidean norm, and $\lambda(k) \in (0,1]$ is the forgetting factor. Minimizing (22) yields

$$\begin{aligned}
\theta^{\mathrm{T}}(k) = \theta^{\mathrm{T}}(k-1) &+ \beta(k)P(k-1)\phi(k-d-1)\\
&\cdot [\phi^{\mathrm{T}}(k-d)P(k-1)\phi(k-d-1) + \lambda(k)]^{-1}\\
&\cdot [\phi^{\mathrm{T}}(k-d-1)\theta^{\mathrm{T}}(k-1) - \hat{u}^{\mathrm{T}}(k-d)],
\end{aligned}$$

where $\beta(k)$ is either zero or one. The error covariance is updated by

$$\begin{aligned}
P(k) = \beta(k)\lambda^{-1}(k)P(k-1) &+ [1-\beta(k)]P(k-1)\\
&- \beta(k)\lambda^{-1}(k)P(k-1)\phi(k-d-1)\\
&\cdot [\phi^{\mathrm{T}}(k-d-1)P(k-1)\phi(k-d) + \lambda(k)]^{-1}\\
&\cdot \phi^{\mathrm{T}}(k-d-1)P(k-1).
\end{aligned}$$

We initialize the error covariance matrix as $P(0) = \alpha(k)I_{3n_{\mathrm{c}}}$, where $\alpha(k) > 0$. Note that when $\beta(k) = 0$, $\theta(k) = \theta(k-1)$ and $P(k) = P(k-1)$. Therefore, setting $\beta(k) = 0$ switches off the controller adaptation, and thus freezes the control gains. When $\beta(k) = 1$, the controller is allowed to adapt.

5 Hysteresis Model

In this paper, we use the rate-dependent Prandtl-Ishlinskii model to represent a class of rate-dependent hysteresis nonlinearity. This model can characterize rate-dependent hysteresis nonlinearity in piezoelectric actuators [5].

5.1 Rate-Dependent Prandtl-Ishlinskii Model

The space of absolutely continuous functions is denoted by $AC(0,T)$. Let the input signal $u(t) \in AC(0,T)$, and let $\rho_i(\dot{u}(t)) \in AC(0,T)$ for all $i \in \{0,1,\ldots,n\}$, where $n \in \mathbb{N}$. Then $\rho_i(\dot{u}(t))$ is chosen such that

$$0 = \rho_0(\dot{u}(t)) \leq \rho_1(\dot{u}(t)) \leq \rho_2(\dot{u}(t)) \leq \cdots \leq \rho_n(\dot{u}(t)). \quad (23)$$

The output $g_i(t)$ of the rate-dependent play operator is denoted as

$$g_i(t) = \Psi_{\rho_i(\dot{u}(t))}[u, x_i](t), \quad (24)$$

for inputs and thresholds that are piecewise linear, that is, linear in each interval of a partition $0 = t_0 < t_1 < \cdots < t_l = T$. The output of the rate-dependent play operator for $t \in (t_{j-1}, t_j]$ can be expressed as

$$g_i(t) = \max\{u(t) - \rho_i(\dot{u}(t)), \min\{u(t) + \rho_i(\dot{u}(t)), g_i(t_{j-1})\}\}, \quad (25)$$

with the initial condition

$$g_i(0) = \max\{u(0) - \rho_i(\dot{u}(0)), \min\{u(0) + \rho_i(\dot{u}(0)), x_i\}\}.$$

The rate-dependent Prandtl-Ishlinskii model is constructed as a superposition of rate-dependent play operators. The output of this model can be expressed as

$$\Phi[u](t) := a_0 u(t) + \sum_{i=1}^{n} a_i \Psi_{\rho_i(\dot{u}(t))}[u, x_i](t), \quad (26)$$

where $a_0, \cdots, a_n$ are positive constants. Next, we define the rate-dependent threshold function

$$\rho_i(\dot{u}(t)) := \zeta_i + \eta_i |\dot{u}(t)|, \quad (27)$$

where ζ_i and η_i are positive constants. The rate-dependent Prandtl-Ishlinskii model specializes to the rate-independent Prandtl-Ishlinskii model when $\eta_i = 0$.

Example 5.1. Consider the sinusoidal command $r(k) = \sin(\omega k)$ with $\omega = \frac{\pi}{30}$ rad/sample and $\omega = \frac{\pi}{3}$ rad/sample, and let $n = 3$, $a_0 = 0.5$, $a_1 = 0.6$, $a_2 = 0.3$, $\zeta_1 = 0.1$, $\zeta_2 = 0.3$, $\eta_1 = 0.8$, and $\eta_2 = 0.5$. The output of the rate-dependent Prandtl-Ishlinskii model is shown in Figure 5. This example shows that the rate-dependent Prandtl-Ishlinskii model can characterize convex, nondecreasing, rate-dependent hysteresis nonlinearities.

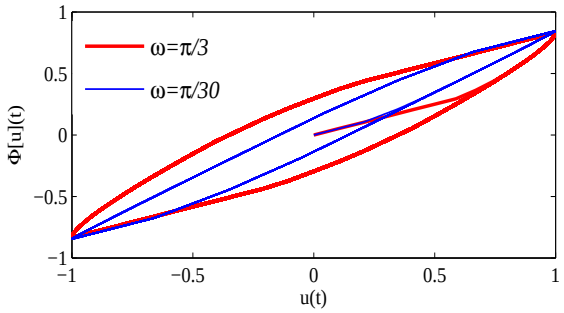

Figure 5. Example 5.1. The output of the rate-dependent Prandtl-Ishlinskii model.

5.2 Modified Rate-Dependent Prandtl-Ishlinskii Model

The rate-dependent Prandtl-Ishlinskii model can be applied to characterize convex rate-dependent hysteresis loops. However, different piezo micro-positioning actuators and magnetostrictive actuators exhibit concave rate-dependent hysteresis nonlinearities that increase as the excitation frequencies of the applied input increases, see for example [1]. In the section we present the modified rate-dependent Prandtl-Ishlinskii model. The output of this modified model is expressed as

$$\Phi_\lambda[u](t) = \Lambda \circ \Phi[u](t) \quad (28)$$

where Λ is a memoryless, continuous, and strictly monotone function. This model can characterize nonconvex, and asymmetrical rate-dependent hysteresis loops. The functions $\Lambda(\upsilon)$ and $\Lambda(-\upsilon)$ of variable $\upsilon \in [0,\infty)$ of deadzone functions expressed as

$$\Lambda(\upsilon) = \sum_{i=0}^{m} \sigma_i S_{\lambda i}(\upsilon) \quad (29)$$

where S_{λ_i} are deadzone functions

$$S_{\lambda_i}(\upsilon) = \max(\upsilon - \lambda_i, 0), \quad (30)$$

σ_i are constants and λ_i are thresholds such that $0 = \lambda_0 \leq \lambda_1 \leq \ldots \leq \lambda_m$.

Example 5.2. Consider rate-dependent Prandtl-Ishlinskii

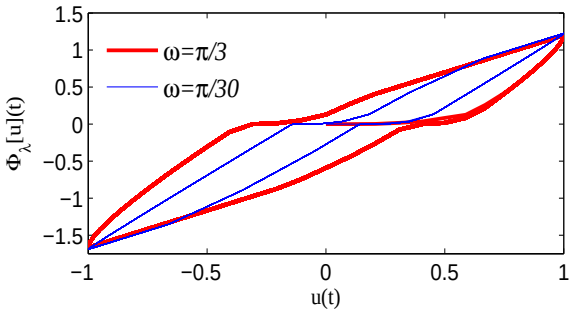

Figure 6. Example 5.3. The output of the modified rate-dependent Prandtl-Ishlinskii model.

model presented in Example 5.1 with $m = 2$, $\lambda_1 = 0.2$, $\lambda_2 = 0.3$, $\sigma_1 = 0.5$, and $\sigma_2 = 0.3$. The output of the modified rate-dependent Prandtl-Ishlinskii model is shown in Figure 6.

5.3 Generalized Rate-Dependent Prandtl-Ishlinskii Model

The rate-dependent model

$$\Phi_\gamma[u](t) = (\Phi \circ \gamma)[u](t) \tag{31}$$

generalizes the rate-dependent Prandtl-Ishlinskii model (26), where γ is a memoryless, continuous, strictly monotonic function.

Example 5.3. Consider rate-dependent Prandtl-Ishlinskii model presented in Example 5.1 with

$$\gamma(u) = 0.93\tanh(1.85u). \tag{32}$$

The output of the generalized rate-dependent Prandtl-Ishlinskii model is shown in Figure 7. The generalized model can characterize rate-dependent hysteresis nonlinearities with saturation.

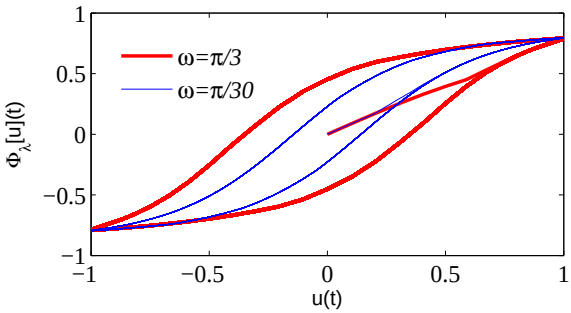

Figure 7. Example 5.3. The output of the generalized rate-dependent Prandtl-Ishlinskii model with $\gamma(u) = 0.93\tanh(1.85u)$.

6 Simulation Results

In this section we assume that the rate-dependent hysteretic input nonlinearity is unknown and cannot be identified. This nonlinearity $\mathcal{N}$ is represented by rate-dependent Prandtl-Ishlinskii models presented in Section 5. The RCAC controller is turned on at $k = 400$.

Example 6.1. We consider the rate-dependent hysteresis nonlinearity of the rate-dependent Prandtl-Ishlinskii model Φ (26) with the minimum-phase unstable plant

$$G(z) = \frac{z-0.99}{z^2+1}. \tag{33}$$

We use the sinusoidal command $r(k) = \sin(\omega k)$ with $\omega = \frac{\pi}{3}$ rad/sample and $\omega = \frac{\pi}{30}$ rad/sample and the disturbance signal of $w(k) = 0.5\sin(\frac{\pi}{3}k)$. We use $n = 3$, $a_0 = 0.5$, $a_1 = 0.25$, $a_2 = 0.125$, $a_3 = 0.0833$, $\zeta_1 = 0.225$, $\zeta_2 = 0.45$, $\zeta_3 = 0.675$, $\eta_1 = \eta_2 = \eta_3 = \frac{1}{3}$. We select $a = 5$, $n_c = 14$, and $P_0 = 1$. Figure 8(a) and 8(b) show the rate-dependent hysteresis nonlinearity at $\omega = \frac{\pi}{3}$ rad/sample and $\omega = \frac{\pi}{30}$ rad/sample, respectively. Figure 8(c) and 8(d) show the resulting time history of the closed-loop performance z with the plant (33). Figure 8(e) shows the closed-loop performance z with the linear plant (33) with the step command $r(k) = 0.7$ and with the disturbance signal $w(k) = 0.5\sin(\frac{\pi}{3}k)$.

Example 6.2. We consider the modified rate-dependent Prandtl-Ishlinskii model (28) and the unstable plant

$$G(z) = \frac{z-0.5}{z^2-1}. \tag{34}$$

We use the sinusoidal command $r(k) = \sin(\omega k)$ with $\omega = \frac{\pi}{3}$ rad/sample and $\omega = \frac{\pi}{30}$ rad/sample and the disturbance signal of $w(k) = 0.75\sin(\pi k)$. We use $n = 3$, $a_0 = 0.6$, $a_1 = 0.25$, $a_2 = 0.125$, $a_3 = 0.0833$, $\zeta_1 = 0.15$, $\zeta_2 = 0.3$, $\zeta_3 = 0.45$, $\eta_1 = \eta_2 = \eta_3 = \frac{1}{3}$, $m = 3$, $\lambda_1 = 0.1$, $\lambda_2 = 0.3$ $\lambda_3 = 0.5$, $\sigma_1 = 0.6$, $\sigma_2 = 0.4$, $\sigma_3 = 1$. We choose $a = 5$, $n_c = 18$, and $P_0 = 2.5$. Figure 9(a) and Figure 9(b) show the rate-dependent hysteresis nonlinearity at $\omega = \frac{2\pi}{7}$ rad/sample and $\omega = \frac{2\pi}{70}$ rad/sample. Figure 9(c) and Figure 9(d) show the resulting time history of the closed-loop performance z with the plant. Figure 9(e) shows the closed-loop response z to the step command $r(k) = 0.5$.

Example 6.3. We consider the generalized rate-dependent Prandtl-Ishlinskii model (31) and the stable non-minimum phase plant

$$G(z) = \frac{z-0.8}{(z-0.9)(z-0.6)}. \tag{35}$$

We use the sinusoidal command $r(k) = \sin(\omega k)$ with $\omega = \frac{\pi}{4}$

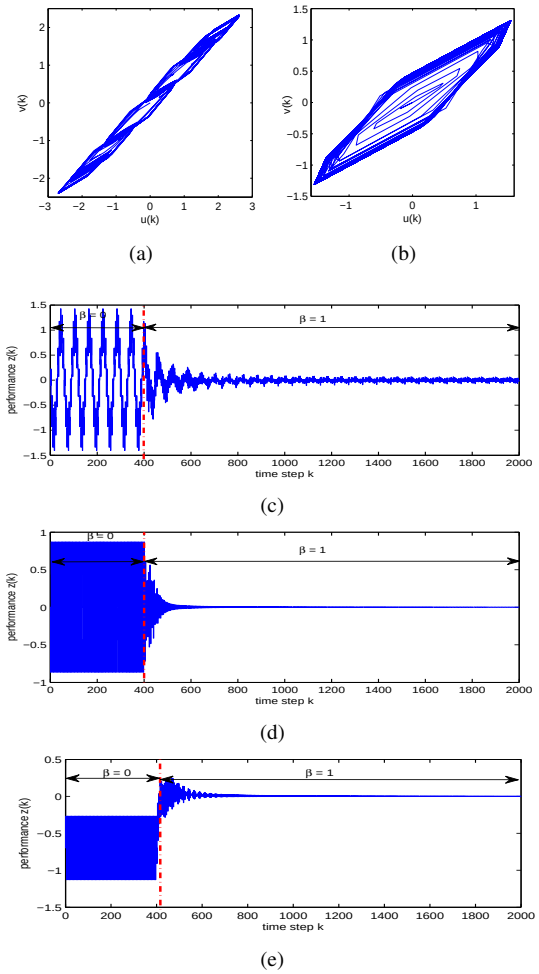

Figure 8. Example 6.1. (a) and (b) show the input nonlinearity $\mathcal{N}(u)$ of the rate-dependent Prandtl-Ishlinskii model with (a) $\omega = \frac{\pi}{3}$ rad/sample, and (b) $\omega = \frac{\pi}{30}$ rad/sample. (c) and (d) show the closed-loop response to the sinusoidal command $r(k) = \sin(\omega k)$ with the plant given by (33) and $w(k) = 0.5\sin(\frac{\pi}{3}k)$. (e) shows the closed-loop response to the step command $r(k) = 0.7$ with the plant given by (33) and $w(k) = 0.5\sin(\frac{\pi}{3}k)$.

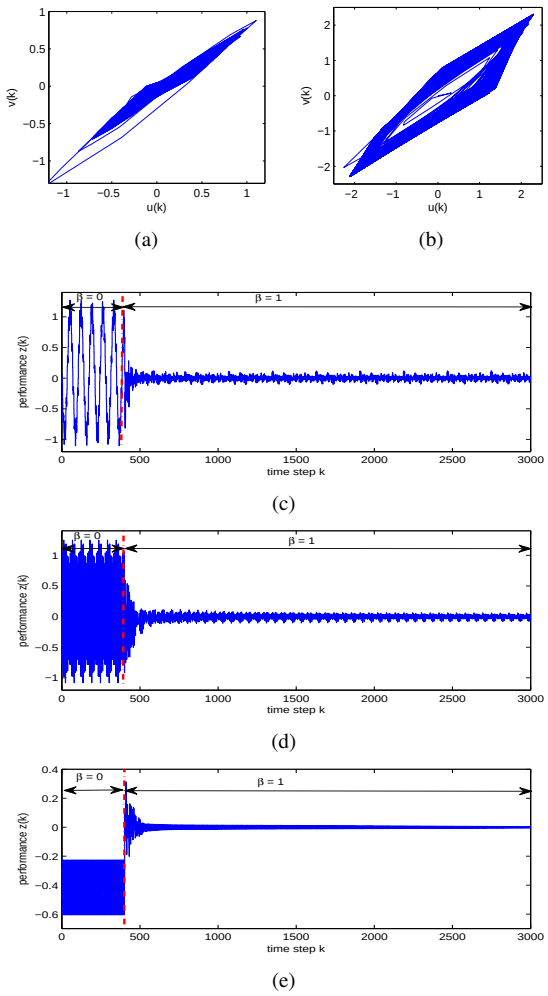

Figure 9. Example 6.2. (a) and (b) show the input nonlinearity $\mathcal{N}(u)$ of the modified rate-dependent Prandtl-Ishlinskii model with :(a) $\omega = \frac{2\pi}{70}$ rad/sample and (b) $\omega = \frac{2\pi}{7}$ rad/sample. (c) and (d) show the closed-loop response to the sinusoidal command $r(k) = \sin(\omega k)$ with the plant given by (34) and $w(k) = 0.5\sin(\frac{\pi}{3})$. (e) shows the closed-loop response to the step command $r(k) = 0.5$ with the linear plant given by (34) and $w(k) = 0.3\sin(\frac{\pi}{4}k)$.

rad/sample and $\omega = \frac{\pi}{40}$ rad/sample and the disturbance signal $w(k) = 0.65\sin(\frac{\pi}{4}k)$. We use $n = 3$, $a_0 = 0.45$, $a_1 = 0.35$, $a_2 = 0.25$, $a_3 = 0.1833$, $\zeta_1 = 0.15$, $\zeta_2 = 0.25$, $\zeta_3 = 0.35$, $\eta_1 = \eta_2 = \eta_3 = 0.5$. We use $a = 4$, $n_c = 8$, and $P_0 = 5$. Figure 10(a) and Figure 10(b) show the rate-dependent hysteresis nonlinearity at $\omega = \frac{\pi}{3}$ rad/sample and $\omega = \frac{\pi}{30}$ rad/sample. Figure 10(c) and Figure 10(d) show the resulting time history of the closed-loop performance z.

Example 6.4. We consider the rate-dependent Prandtl-Ishlinskii model (26) and the linear plant

$$G(z) = \frac{z+1}{z^2+1.4z+0.8}. \tag{36}$$

We use the sinusoidal command $r(k) = 1.3\sin(0.5\omega k) + 0.65\sin(\omega k)$ with $\omega = \frac{\pi}{4}$ rad/sample and the disturbance signal of $w(k) = 0.5\sin(\frac{\pi}{3}k)$. We use $n = 3$, $a_0 = 0.75$, $a_1 = 0.35$, $a_2 = 0.15$, $a_3 = 0.095$, $\zeta_1 = 0.3$, $\zeta_2 = 0.4$, $\zeta_3 = 0.5$, $\eta_i = i\eta$, where η is a positive constant determines the rate-dependency hysteretic nonlinearities. We use $a = 7$, $n_c = 18$, and $P_0 = 0.5$. Figure Figure 11(a) and Figure 11(b) show the hysteresis nonlinearity with $\eta = 1$ and $\eta = 0$, respectively. Figure 11(c) and Figure 11(d) show the resulting time history of the closed-loop performance z.

Example 6.5. We consider the rate-dependent hysteresis nonlinearity with the linear plant (36) presented in Example (6.4). In order to show the robustness of the RCAC con-

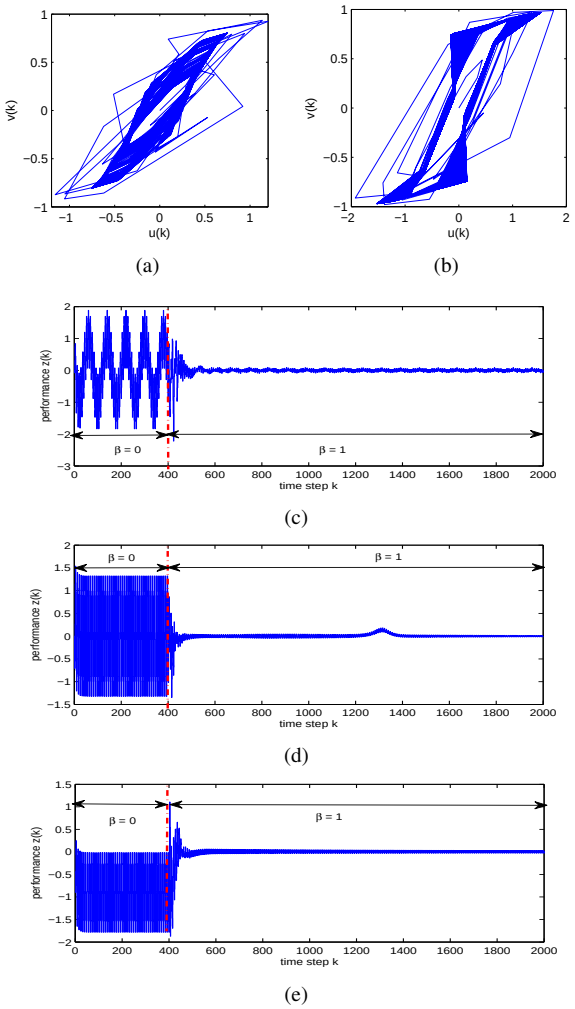

Figure 10. Example 6.3. (a) and (b) show the input nonlinearity $\mathcal{N}(u)$ of the rate-dependent Prandtl-Ishlinskii model for the sinusoidal command $r(k) = \sin(\omega k)$ with the plant given by (35) and $w(k) = 0.65\sin(\frac{\pi}{4}k)$ (a) $\omega = \frac{\pi}{4}$ rad/sample, and (b) $\omega = \frac{\pi}{40}$ rad/sample. (c) show the closed-loop response with (a), (d)show the closed-loop response with (b). (e) shows the closed-loop response to the sinusoidal command $r(k) = 0.9$ with the plant given by (35) and $w(k) = 0.5\sin(\frac{\pi}{3}k)$.

troller, we present the closed-loop response z when $\hat{H}_d = 2$ with $\omega = \frac{\pi}{4}$ rad/sample and $\omega = \frac{\pi}{40}$ rad/sample. Figure 12(c) and Figure12(d) show the closed-loop response z when $\hat{H}_d = 2$ and $\hat{H}_d = 1$ with $r(k) = 1$ and $w(k) = 0.25\sin(\frac{\pi}{3}k)$.

7 CONCLUSIONS

Retrospective cost adaptive control (RCAC) was applied to a command-following problem for Hammerstein systems with rate-dependent hysteretic input nonlinearity modeled with the rate-dependent Prandtl-Ishlinskii model. We considered the following input nonlinearities: (i) rate-independent and rate-dependent hysteresis nonlinearities, and (ii) convex and nonconvex hysteresis loops. RCAC was used with limited modeling information about the hysteretic systems. In particular, RCAC uses knowledge of only the first nonzero Markov parameter of the linear system. RCAC was able to drive the Hammerstein system to follow the reference command when the linear plant was asymptotically stable or unstable. Finally, these results show that RCAC can be used to control systems consisting of a smart actuator followed by a linear plant without using the estimated inverse model as a feedforward compensator in the closed-loop control system.

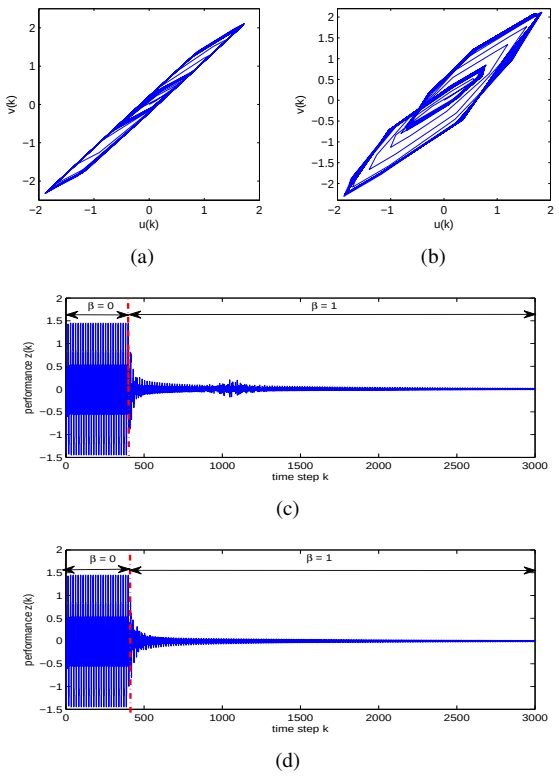

Figure 11. Example 6.4. (a) and (b) show the input nonlinearity $\mathcal{N}(u)$ of the rate-dependent Prandtl-Ishlinskii model with (a) $\eta = 1$, and (b) $\eta = 0$. (c) and (d) show the closed-loop response to the sinusoidal command $r(k) = 1.3\sin(0.5\omega k) + 0.65\sin(\omega k)$ with $\omega = \frac{\pi}{4}$ rad/sample with the plant given by (36) and $w(k) = 0.5\sin(\frac{\pi}{3}k)$ when (c) $\eta = 0$, and (d) $\eta = 1$.

REFERENCES

[1] R. C. Smith, *Smart Material Systems*. Philadelphia, PA: Springler-Verlag, 2005.

[2] Y. Li and Q. Xu, "A Totally Decoupled Piezo-Driven XYZ Flexure Parallel Micropositioning Stage for Micro/Nanomanipulation," *IEEE Transactions on Automation Science and Engineering*, vol. 8, no. 2, pp. 265-279, April 2011.

[3] K. K. Leang, Q. Zou and S. Devasia, "Feedforward Control

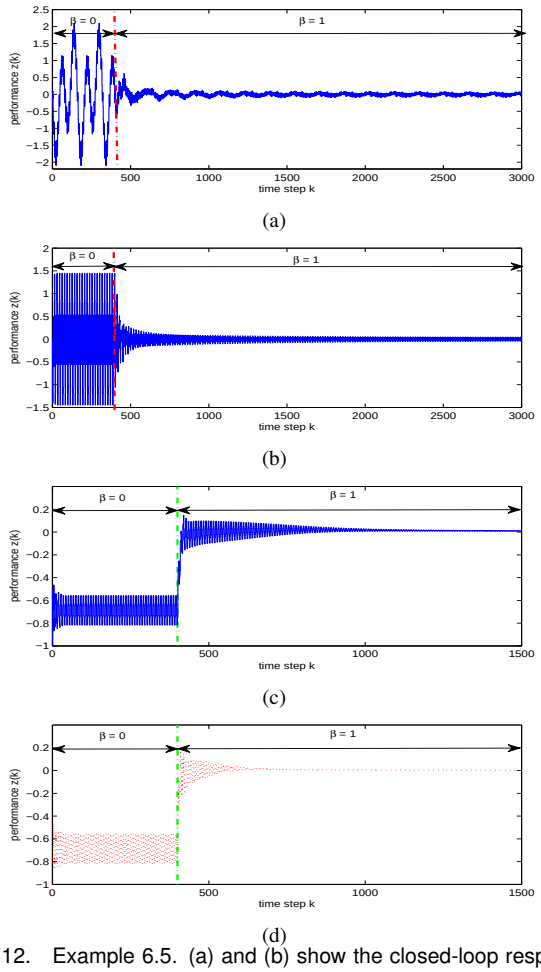

Figure 12. Example 6.5. (a) and (b) show the closed-loop response to the sinusoidal command $r(k) = 1.3\sin(0.5\omega k) + 0.65\sin(\omega k)$ with $\hat{H}_d = 2$ and $w(k) = 0.5\sin(\frac{\pi}{3}k)$: (a) $\omega = \frac{\pi}{4}$ rad/sample, and (b) $\omega = \frac{\pi}{40}$ rad/sample. (c) shows the closed-loop response to the command signal $r(k) = 1$ with the disturbance signal $w(k) = 0.2\sin(0.5\pi k)$ considering (c) $\hat{H}_d = 2$, and (d) $\hat{H}_d = 1$.

of Piezoactuators in Atomic Force Microscope Systems," *IEEE Contr. Sys. Mag.*, vol. 29, pp. 70–82, 2009.

[4] M. Brokate and J. Sprekels, *Hysteresis and Phase Transitions*. Springler, 1994.

[5] M. Al Janaideh, S. Rakheja, and C-Y. Su, "Experimental characterization and modeling of rate-dependent hysteresis of a piezoceramic actuator," *Mechatronics*, vol. 17, no. 5, pp. 656-670, 2009.

[6] R. V. Iyer, X. Tan and P. S. Krishnaprasad, "Approximate inversion of the Preisach hysteresis operator with applications to control of smart actuators," *IEEE Trans. Autom. Contr.*, vol. 50, no. 6, pp. 798-810, 2005.

[7] A. G. Hatch, R. C. Smith, T. De and M. V. Salapaka, "Construction and Experimental Implementation of a Model-Based Inverse Filter to Attenuate Hysteresis in Ferroelectric Transducers," *IEEE Trans. Contr. Sys. Tech.*, vol. 14, pp. 1058-1069, 2006.

[8] G. Tao and P. V. Kokotović, *Adaptive Control of Systems with Actuator and Sensor Nonlinearities*. New York: Wiley, 1996.

[9] X. Tan and J. Baras, "Modeling and control of hysteresis in magnetostrictive actuators", *Automatica*, vol. 40, no. 9, pp. 1469–1480, 2004.

[10] C-Y. Su, Y. Feng, H. Hong and X. Chen, "Adaptive control of systems involving complex hysteretic nonlinearities: a generalized Prandtl-Ishlinskii modeling approach," *Int. J. of Control*, vol. 82, no. 10, pp. 1786-1793, 2009.

[11] R. Venugopal and D. S. Bernstein, "Adaptive disturbance rejection using ARMARKOV system representations," *IEEE Trans. Contr. Sys. Tech.*, Vol. 8, pp. 257-269, 2000.

[12] J. B. Hoagg, M. A. Santillo, and D. S. Bernstein, "Discrete-time adaptive command following and disturbance rejection for minimum phase systems with unknown exogenous dynamics," *IEEE Trans. Autom. Contr.*, vol. 53, pp. 912-928, 2008.

[13] M. A. Santillo and D. S. Bernstein, "Adaptive Control Based on Retrospective Cost Optimization," *AIAA J. Guid. Contr. Dyn.*, vol. 33, pp. 289–304, 2010.

[14] J. B. Hoagg and D. S. Bernstein, "Retrospective Cost Adaptive Control for Nonminimum-Phase Discrete-Time Systems Part 1: The Ideal Controller and Error System; Part 2: The Adaptive Controller and Stability Analysis," *Proc. Conf. Dec. Contr.*, pp. 893–904, Atlanta, GA, December 2010.

[15] J. B. Hoagg and D. S. Bernstein, "Retrospective Cost Model Reference Adaptive Control for Nonminimum-Phase Discrete-Time Systems, Part 1: The Adaptive Controller; Part 2: Stability Analysis," *Proc. Amer. Contr. Conf.*, pp. 2927–2938, San Francisco, CA, June 2011.

[16] A. M. D'Amato, E. D. Sumer, and D. S. Bernstein, "Retrospective Cost Adaptive Control for Systems with Unknown Nonminimum-Phase Zeros," AIAA Guid. Nav. Contr. Conf., Portland, OR, August 2011, AIAA-2011-6203.

[17] A. M. D'Amato, E. D. Sumer, and D. S. Bernstein, "Frequency-Domain Stability Analysis of Retrospective-Cost Adaptive Control for Systems with Unknown Nonminimum-Phase Zeros," *Proc. Conf. Dec. Contr.*, pp. 1098-1103, Orlando, FL, December 2011.

[18] J. Yan, A. M. D'Amato, D. Sumer, J. B. Hoagg, and D. S. Bernstein, "Adaptive Control of Uncertain Hammerstein Systems Using Auxiliary Nonlinearities" submitted to *Proc. Conference on Decision and Control*, Maui, Hawaii, December 2012.

[19] P. Krejčí, M. Al Janaideh and F. Deasy, "Inversion of hysteresis and creep operators," *Physica B*, vol. 407, pp. 1354-1356, 2012.

[20] M. Al Janaideh and P. Krejčí , "Prandtl-Ishlinskii hysteresis models for complex time dependent hysteresis nonlinearities," *Physica B*, vol. 407, pp. 1365-1367, 2012.